

# Dynamic Modeling and Experimental Evaluation of Olefin Copolymerization with Vanadium-Based Catalysts

Mohammad Reza Pourhossaini,<sup>1</sup> Ebrahim Vasheghani-Farahani,<sup>1</sup> Maryam Gholamian,<sup>2</sup> Mahmood Gholamian<sup>2</sup>

<sup>1</sup>Chemical Engineering Department, Tarbiat Modares University, P.O. Box 14115-143, Tehran, Iran

<sup>2</sup>Research Institute of Petroleum Industry, P.O. Box 18745-4163, Tehran, Iran

Received 4 May 2004; accepted 10 December 2004

DOI 10.1002/app.22473

Published online in Wiley InterScience (www.interscience.wiley.com).

**ABSTRACT:** In this study, we developed a mathematical model for olefin copolymerization using soluble Ziegler–Natta catalysts in a semibatch reactor to predict the reaction rate and polymer characteristics (i.e., molecular weight, polydispersity, and ethylene content) as functions of the reaction parameters (i.e., time, temperature, pressure, concentrations, and so on) accurately. The proposed model differs from others because it considers the olefin copolymerization as a dynamic process and applies double moments for two reactants (ethylene and propylene) in the presence of hydrogen. To establish the model validity, the

copolymerization was performed with  $\text{VOCl}_3\text{--Al}_2\text{Et}_3\text{Cl}_3$  systems with hydrogen as a molecular weight controlling agent. The dynamic model was able to reproduce the experimental data within experimental accuracy and accurately demonstrated the fundamental importance of the polymerization variables on the final properties of the polymer material in the copolymerization of ethylene and propylene with Al/V ratios of up to 28 before synthesis. © 2006 Wiley Periodicals, Inc. *J Appl Polym Sci* 100: 3101–3110, 2006

**Key words:** catalysts; copolymerization; kinetics (polym.)

## INTRODUCTION

The intrinsic complexity of olefin copolymerization with Ziegler–Natta catalysts demands reaction models to control and better understand the polymerization process. The Ziegler–Natta process is one of the most studied polymerization systems for modeling,<sup>1–17</sup> and several reviews on olefin polymerization with Ziegler–Natta catalysts are available in the literature.<sup>18–26</sup>

In ethylene–propylene copolymerization, Podolnyi et al.<sup>1</sup> investigated the effect of 2-ethylidene-cyclo[2.2.1]hept-5-ene with  $\text{VOCl}_3\text{--Al}_2\text{Et}_3\text{Cl}_3$ , applying a batch system under a constant monomer pressure. They assumed that all reactions occurred instantaneously, and they observed a higher reactivity for ethylene and its terminated chains with 2-ethylidene-cyclo[2.2.1]hept-5-ene. Pronyaev et al.<sup>2</sup> studied ethylene–propylene copolymerization kinetics, applying a  $\text{VOCl}_3\text{--Al}_2\text{Et}_3\text{Cl}_3$  system with an experimental unit identical to the one used by Podolnyi et al.<sup>1</sup> by considering chain-transfer reactions and the activation or

deactivation of the catalyst by the monomers. They concluded that the activation and deactivation rates were very similar. The number of active centers was around 15–40% of the initial  $\text{VOCl}_3$  concentration. Pronyaev et al.<sup>2</sup> and Podolnyi et al.<sup>1</sup> presented simplified mathematical models to determine the kinetic constants. Nevertheless, neither reported the detailed set of reaction equations used in the model for olefin copolymerization.

Cozewith<sup>3</sup> built a more complex kinetic model of the copolymerization reaction with a vanadium salt–alkylaluminum catalyst and verified the influence of Al/V ratio on molecular weight under different catalytic systems. He concluded that polymeric chain lifetime was not instantaneous, as previously proposed by Podolnyi et al.,<sup>1</sup> but it was on the order of minutes. Cozewith<sup>4</sup> also studied the influence of hydrogen on the molecular weight with the  $\text{VOCl}_3\text{--Al}_2\text{Et}_3\text{Cl}_3$  catalytic system for ethylene–propylene copolymerization in a continuous stirred tank reactor (CSTR) reactor. To produce monodisperse polymers, he modeled the ethylene–propylene copolymerization with a plug flow reactor in a later study.<sup>5</sup> He observed that the compositional distribution was not homogeneous because of the ethylene–propylene ratio variation (composition drift) in the reactor because ethylene is more reactive than propylene.

Haag et al.<sup>6</sup> proposed a dynamic model based on the method of single moments with some simplifications to describe influence of Al/V ratio and diene

Correspondence to: E. Vasheghani-Farahani (evf@modares.ac.ir).

Contract grant sponsor: National Petrochemical Co.

Contract grant sponsor: Research Institute of Petroleum Industry of Iran.

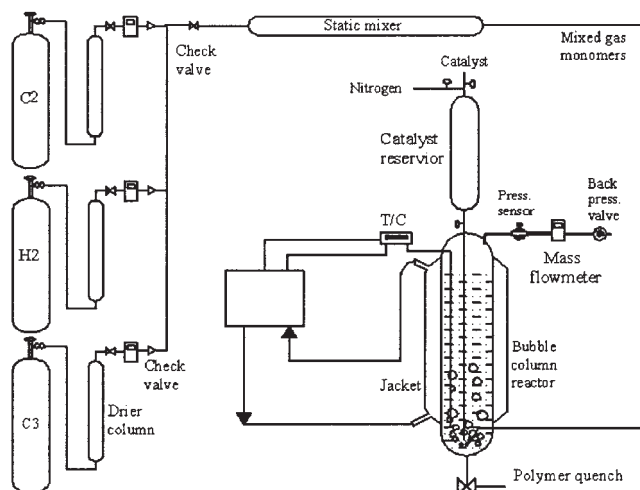


Figure 1 Schematic view of the polymerization system.

concentration on the reaction yield and polymer characteristics such as molecular weight, polydispersity index (PDI), and ethylene incorporation.

da Silva Filho et al.<sup>7</sup> and Soares<sup>8</sup> carried out more investigations to develop mathematical models to describe the microstructure of polyolefins produced by coordination polymerization.

Recently, Latado et al.<sup>9</sup> developed empirical models to predict the end-use properties of poly(ethylene-propylene) resins as functions of the more fundamental molecular and morphological properties of the polymer resins. The final properties analyzed were two mechanical properties, rigidity and impact strength, and one thermal property, glass-transition temperature. Two additional properties of practical importance were also modeled: the melt index and the xylene soluble content. The molecular and morphological properties selected for resin characterization were molecular weight distribution, polymer composition, rubbery phase dispersion, spherulite size distribution, and degree of crystallinity.

In this study, we focused on the mathematical modeling of olefin copolymerization with vanadium catalyzed with a semibatch bubble column reactor to describe the microstructure of the resulting copolymer

chains. The proposed model differs not only from the one developed by Podolnyi et al.<sup>1</sup> by considering the olefin copolymerization as a dynamic process but also from those developed by da Silva Filho et al.,<sup>7</sup> Soares,<sup>8</sup> Haag et al.,<sup>6</sup> and Latado et al.<sup>9</sup> by applying double moments for two reactants, ethylene and propylene, to accurately describe the influence of hydrogen and Al/V ratio on the copolymer characteristics (i.e., molecular weight, dispersity, and ethylene content) as functions of the reaction parameters.

## EXPERIMENTAL

### Chemicals

Ethylene and propylene monomers were purchased from Arak Petrochemical Company (Arak, Iran) (polymerization grade); both had a purity of 99.9% or greater. Heptane (>99%),  $\text{VOCl}_3$  (>99.5%), and the solvated cocatalyst  $\text{Al}_2\text{Et}_3\text{Cl}_3$  (97%) were bought from Merck Co. (Haar, Germany).

### Polymerization system

The polymerization unit is shown in Figure 1. The solution polymerization reaction was carried out in a 300-mL semibatch bubble column reactor (stainless steel) with *n*-heptane as the solvent. The liquid phase (solvent, catalyst, and cocatalyst) was operated in batch to guarantee a constant feed composition in the reaction medium and to produce a homogeneous copolymer.

At first, the monomers and hydrogen (the gas phase) with specified ratios (Table I) were fed continuously at a constant rate to saturate the solvent in the reactor. The vanadium compound ( $\text{VOCl}_3$ ) and the required amount of cocatalyst ( $\text{Al}_2\text{Et}_3\text{Cl}_3$ ) were introduced into a glass reservoir containing *n*-heptane (10–15 mL) at 25°C under a positive pressure of nitrogen (Table I). Then, under a constant pressure ( $1 \pm 0.1$  atm) and at a constant temperature ( $22 \pm 1^\circ\text{C}$ ), the reaction was initiated with a one-shot injection of the aged catalyst at its highest activity into the reactor, and gas-phase feeding continued the reaction for 90

TABLE I  
Operational Conditions Used to Synthesize Ethylene–Propylene Copolymers with Desirable Properties

Concentration/ratio	Value	Initial condition	Value
$\text{VOCl}_3$ (mol/L)	$7.2 \times 10^{-5}$	$T_{\text{SET}}$ ( $^\circ\text{C}$ )	22
$\text{Al}_0/\text{C}_{10}$	28.680	$P_{\text{SET(ABS)}}$ (bar)	2
$H_S$ (mol/L)	0.048	$F_E$ (L/min)	0.016
$E_S$ (mol/L)	0.021	$F_P$ (L/min)	0.050
$P_S$ (mol/L)	0.411	$F_H$ (L/min)	0.115
[Propylene]/[Ethylene]	19.048	$V_L$ (cc)	250

$T_{\text{SET}}$ , temperature set point;  $P_{\text{SET}}$ , pressure set point.

TABLE II  
Catalyzed Olefin Copolymerization Kinetic Model

Reaction type	Agent	Kinetic constant	Reaction
Activation		$k_a$	$C_1 \xrightarrow{k_a} C_2$
Deactivation	Poison	$k_x$	$C_2 \xrightarrow{k_x} D$
Chain initiation	E	$k_{i1}$	$C_2 + E \xrightarrow{k_{i1}} E_{1,0}$
	P	$k_{i2}$	$C_2 + P \xrightarrow{k_{i2}} P_{0,1}$
Chain propagation	E	$k_{11}$	$E_{i,j} + E \xrightarrow{k_{11}} E_{i+1,j}$
		$k_{12}$	$E_{i,j} + P \xrightarrow{k_{12}} P_{i,j+1}$
	P	$k_{21}$	$P_{i,j} + E \xrightarrow{k_{21}} E_{i+1,j}$
		$k_{22}$	$P_{i,j} + P \xrightarrow{k_{22}} P_{i,j+1}$
Chain transfer <sup>a</sup>	P	$k_{tr12}$	$E_{i,j} + P \xrightarrow{k_{tr12}} OCP_{i,j} + P_{0,1}$
	Al-alkyl	$k_{tr1Al}$	$E_{i,j} + Al \xrightarrow{k_{tr1Al}} OCP_{i,j} + E_{1,0}$
	Hydrogen	$k_{tr1H}$	$E_{i,j} + H \xrightarrow{k_{tr1H}} OCP_{i,j} + C_2$
Chain termination <sup>a</sup>	Deactivation	$k_{ter1}$	$E_{i,j} \xrightarrow{k_{ter1}} OCP_{i,j} + D$
	P	$k_{ter12}$	$E_{i,j} + P \xrightarrow{k_{ter12}} OCP_{i,j+1} + D$

E, ethylene; P, propylene; OCP, olefin copolymer.

<sup>a</sup> Identical reactions occurred with growing  $P_{i,j}$  chains to produce dead  $OCP_{i,j}$  chains. Termination and transfer constants were assumed to be the same, regardless of the chain end type.<sup>4</sup>

min, when the resulting reaction medium contained 2 wt % or less of the soluble copolymer, to prevent rheological effect on the kinetics. During the reaction, the reactor was maintained at a constant pressure, and excess monomers were vented off by a manually controlled back-pressure regulator. At the end of the reaction, the feed streams were shut off, and isopropyl alcohol was added to quench the reaction and to precipitate the soluble polymer. Then, the precipitated polymer was separated, washed with excess isopropyl alcohol, and vacuum-dried at 40–70°C for 24 h.

One factor variation at a time is the design of the many kinetic experiments; we applied this design to study the effect of the 11 key factors (at least at four levels) on the resulting copolymer properties with regard to the catalyst system and operation conditions, as suggested by Natta et al.<sup>18</sup> Each experiment was repeated enough times to ensure the reproducibility of the results. Finally, the best conditions were chosen to produce low-molecular-weight and monodisperse olefin copolymers as viscosity modifiers in engine oil, and these were used in the model computations and model evaluation experiments, as shown in Table I.

### Copolymer characterization

We characterized the polymer films (0.18–0.2 mm) for ethylene incorporation with IR spectroscopy (PerkinElmer 2100, Boston, MA) by measuring the

ratio of the intensities of the 1155-cm<sup>-1</sup> methyl band and the 720-cm<sup>-1</sup> methylene band according to ASTM D 3900.

<sup>13</sup>C-NMR (Bruker ACP 500 MHz, Midland, Canada) in CDCl<sub>3</sub> at 50°C was used to more accurately identify the ethylene content of the synthesized copolymer.<sup>10–14</sup>

The molecular weights and their distributions were determined by gel permeation chromatography (Waters 150C ALC/GPC) in tetrahydrofuran at 50°C. The data were analyzed with polystyrene calibration curves.

The specific heat capacity of the copolymer was determined with differential scanning calorimetry (12000 PL-DSC) at a heating rate of 10°C/min.

## MODEL DEVELOPMENT

### Theoretical kinetic scheme

VOCl<sub>3</sub>–Al<sub>2</sub>Et<sub>3</sub>Cl<sub>3</sub> created a soluble Ziegler–Natta catalyst system with a single active site, which was suitable for the generation of a monodisperse copolymer with a homogeneous copolymer composition. The accepted mechanism for Ziegler–Natta copolymerization is given in Table II.<sup>6</sup> Most of the reactions presented bimolecular kinetics, except those concerning the catalyst activation or deactivation and chain spontaneous termination.

The catalyst ( $C_1$ , whose concentration is  $C_1$ ) had to undergo activation by the alkyl cocatalyst in a rapid

and complete reaction or it might have been deactivated by a spontaneous reaction.

In this system, chain growth began with the initiation step due to ethylene and propylene, as assumed previously by Cozewith.<sup>4</sup> Chain growth was followed by rapid chain propagation, resulting from the combination of both monomers, which theoretically generated four equations in the propagation step.

The chain-transfer step contained transfer reactions to propylene, excess alkyl, and hydrogen. In olefin copolymerizations, ethylene shows the highest reactivity in propagation step. If the ethylene monomer faces any live polymer chain, it will display propagation behavior rather than transfer or termination. Thus, ethylene exhibited a negligible tendency toward chain-transfer reactions, and the chain transfer to propylene was more important, which itself had little effect on the molecular weight. So, chain-transfer reactions to the monomers occurred only because of propylene with little efficiency to govern molecular weight. The propylene chain-transfer reaction formed a dead polymer chain ( $OCP_{i,j}$ ) and a live polymer unitary chain ( $E_{i,j}$ ) or ( $P_{i,j}$ ). Hydrogen and excess alkyl created a dead polymer chain ( $OCP_{i,j}$ ) and a vacant site, which are considered in the proposed model, and hydrogen basically controlled the polymer molecular weight.<sup>4,6</sup>

The mechanisms of site deactivation occurred due to propylene ( $k_{ter12}$ ; see Table II for descriptions of all of the kinetic constants used in this article) or spontaneously ( $k_{ter1}$ ). In both cases, they created permanently deactivated sites ( $D$ 's, whose concentrations are  $D$ 's) followed by the termination of the growing polymer chain ( $OCP_{i,j}$ ).<sup>4,6</sup>

The standard Ziegler–Natta scheme does not account for branching reactions. Branching is the result of the generated internal and terminal double bonds in polymer chains. Other effective cause of double bond generation is  $\beta$ -hydride elimination. However, this reaction is not included in our model because no double bond effects are detected in synthesized copolymer with infrared spectroscopy<sup>5</sup> or <sup>13</sup>C-NMRIO-14.

### Mass balance

We considered the mass balance for both the liquid and gas phases separately. Indices  $G$  and  $L$  were assigned to gas and liquid phases, respectively. We assumed that only the monomer in the liquid phase was capable of participating in the polymerization; hence, the reaction took place only in the liquid phase. Equations of the population balance described the variation in the concentration of the active species with time in the liquid phase during polymerization. These equations were derived for live and dead polymer chains in the semibatch bubble column reactor.

### Gas-phase mass balance

The mass balance for each component in the gas phase including ethylene, propylene, and hydrogen was calculated as described by Hagg et al.<sup>6</sup> The resulting equations for the accumulation of gases in the gas phase are as follows:

$$\frac{dE_G}{dt} = \frac{F_E}{V_G} E_F - k_l a_E \frac{V_L}{V_G} (E_{EQ} - E_S) - \frac{F_G}{V_G} E_{GS} \quad (1)$$

$$\frac{dP_G}{dt} = \frac{F_P}{V_G} P_F - k_l a_P \frac{V_L}{V_G} (P_{EQ} - P_S) - \frac{F_G}{V_G} P_{GS} \quad (2)$$

$$\frac{dH_G}{dt} = \frac{F_H}{V_G} H_F - k_l a_H \frac{V_L}{V_G} (H_{EQ} - H_S) - \frac{F_G}{V_G} H_{GS} \quad (3)$$

where  $E_G$ ,  $E_F$ ,  $E_{EQ}$ ,  $E_{GS}$ , and  $E_S$  are the ethylene concentrations in the gas phase, in the feed, at equilibrium, released by the pressure control valve (gas out), and solved in the liquid phase, respectively;  $V_G$  and  $V_L$  are the volumes of the gas and liquid phases, respectively;  $F_E$ ,  $F_G$ ,  $F_P$ , and  $F_H$  are the volumetric flow rates of ethylene, the gas phase, propylene, and hydrogen, respectively;  $k_l$  is the mass-transfer coefficient based on the liquid phase for ethylene, propylene, or hydrogen;  $a_E$ ,  $a_P$ , and  $a_H$  are the interfacial specific areas of ethylene, propylene, and hydrogen, respectively;  $P_G$ ,  $P_F$ ,  $P_{EQ}$ ,  $P_S$ , and  $P_{GS}$  are the propylene concentrations in the gas phase, in the feed, at equilibrium, solved in the liquid phase, and released by the control valve, respectively; and  $H_G$ ,  $H_F$ ,  $H_{EQ}$ ,  $H_S$ , and  $H_{GS}$  are the hydrogen concentrations in the gas phase, in the feed, at equilibrium, solved in the liquid phase, and released by the control valve, respectively. The necessary data were estimated with the standard procedure for bubble column reactors.<sup>27</sup>

### Liquid-phase mass balance

Catalyst, cocatalyst, monomers, live and dead polymeric chains, and the solvent were considered when we calculated the mass balance in the liquid phase. In the case of copolymerization, two indices are necessary to define the polymerization degree of each live or dead chain. At any instance, a live polymer is shown by  $\lambda_{i,j}^E$ , where  $\lambda$  signifies live chains,  $i$  is the total number of ethylene units and  $j$  is the total number of propylene units that are incorporated into the copolymer structure, and the superscript  $E$  indicates that the last unit of the live chain is ethylene. This terminology satisfies the following assumptions:

1. The reaction medium is saturated by both monomers before reaction initiation. The mass-transfer rates of both monomers are higher than the polymerization rates in magnitude (reaction-controlled process).



2. The active site of each monomer initiates and propagates at different rates.

3. Cozewith<sup>3</sup> pointed out that chain building time is on the order of 1–3 min; therefore, the quasi-steady-state approach does not apply in the proposed model:

$$\frac{d\lambda_{ij}^M}{dt} \neq 0 \quad (4)$$

The active chain ( $M_{n,m}$ ) and dead polymer chain ( $OCP_{n,m}$ ) moments of the  $i,j$ th orders are defined according to eq. (5):

$$M_{n,m} \Rightarrow \lambda_{ij}^M = \sum_{n=0}^{\infty} \sum_{m=0}^{\infty} (n^i m^j M_{n,m}) \quad (5)$$

$$OCP_{n,m} \Rightarrow \mu_{ij} = \sum_{n=0}^{\infty} \sum_{m=0}^{\infty} (n^i m^j OCP_{n,m})$$

where  $m$  is the number of ethylene units,  $n$  is the number of propylene units, and  $\mu_{ij}$  is the order of double moments for the dead chains.

Deactivation is composed of vanadium oxide formation and poisoning.<sup>28</sup> These reactions [eq. (6)] deactivated 1% of the total amount of the catalyst. Thus, this information was incorporated into the model as a correction for catalyst concentration:

$$\frac{dD}{dt} = k_x C_1 \quad (6)$$

Not only the activation reaction but also deactivation reaction decreases the concentration of nonactivated catalyst ( $C_1$ ), as given in the following equation:

$$\frac{dC_1}{dt} = - (k_x + k_a) C_1 \quad (7)$$

Active species ( $C_2$ , whose concentration is  $C_2$ ) are formed by activation and hydrogen chain-transfer reaction, and they are consumed in the initiation step of both monomers:

$$\frac{dC_2}{dt} = k_a C_1 - (k_{i1} E_S + k_{i2} P_S) C_2 + k_{trH} H_S \lambda_{0,0}^E \quad (8)$$

Transfer reactions reduce the initial alkyl aluminum concentration. One obtains the transfer reaction rate with alkyl aluminum by replacing the aluminum concentration with the ratio of alkyl aluminum ethyl bonds to vanadium, which are calculated with the assumption that the vanadium catalyst is reduced to a valance of three during catalyst activation and that one alkyl group reduces one vanadium by one valance

unit.<sup>4</sup> Hence, the effect of the alkyl chain-transfer reaction on the activated monomer ( $\lambda_{0,0}^E$ ) is given by

$$\frac{dAl}{dt} = - k_{tr12} \left( \frac{Al_0}{C_{10}} - 1 \right) Al_0 \lambda_{0,0}^E \quad (9)$$

where  $Al$  is the initial alkyl aluminum concentration and  $Al_0$  and  $C_{10}$  are the corrected catalyst and cocatalyst concentrations, respectively, after the poisoning effect is incorporated.

The concentration of monomers can be expressed on the basis of mass transfer from the gas phase to the liquid phase by convection and monomer consumption in the initiation and propagation steps:

$$\frac{dE_S}{dt} = 0 = k_{tE} a_E \frac{V_L}{V_G} (E_{EQ} - E_S) - (k_{i1} C_2 + k_{11} \lambda_{0,0}^E + k_{21} \lambda_{0,0}^P) E_S \quad (10)$$

$$\frac{dP_S}{dt} = 0 = k_{tP} a_P \frac{V_L}{V_G} (P_{EQ} - P_S) - [k_{i2} C_2 + k_{12} \lambda_{0,0}^E + k_{22} \lambda_{0,0}^P + (k_{tr12} + k_{ter12}) \lambda_{0,0}^E] P_S \quad (11)$$

$$\frac{dH_S}{dt} = 0 = k_{tH} a_H \frac{V_L}{V_G} (H_{EQ} - H_S) - k_{trH} (\lambda_{0,0}^P + \lambda_{0,0}^E) H_S \quad (12)$$

The equilibrium monomer concentrations were obtained from a correlation given by Kissin.<sup>28</sup> The hydrogen equilibrium concentration was computed (at experimental conditions) by the total monomer pressures as the equilibrium criterion and group contribution equation of state, the predictive Soave–Redlich–Kwong equation.<sup>29,30</sup> This method is based on the universal quasichemical functional group activity coefficients (UNIFAC) model, which has been verified by experimental data for many gaseous compounds, such as light hydrocarbons and hydrogen.<sup>29,30</sup> The calculated solubility values of the monomers and hydrogen were close to the experimental data reported by Stephen and Stephen,<sup>31</sup> with a 0.5% relative deviation.

During the reaction, the concentrations of live polymeric chains terminated with ethylene and propylene were given by

$$\frac{d\lambda_{0,0}^E}{dt} = k_{i1} C_2 E_S + k_{21} E_S \lambda_{0,0}^P - [\alpha - \beta] \lambda_{0,0}^E \quad (13)$$

$$\frac{d\lambda_{0,0}^P}{dt} = k_{i2} C_2 P_S + (k_{12} + k_{tr12}) P_S \lambda_{0,0}^E - (\gamma + \varepsilon - \phi) \lambda_{0,0}^P \quad (14)$$

where  $\alpha$ ,  $\beta$ ,  $\gamma$ ,  $\varepsilon$ , and  $\phi$  are mathematical variables of the model and are defined as

**TABLE III**  
**Moments Balance Equations of the Kinetic Model for Live and Dead Copolymer Chains**

Moment balance equations of different orders	
Live copolymer chains with an ethylene unit at the end	$\frac{d\lambda_{0,1}^E}{dt} = k_{i1}C_2E_S + k_{21}E_S\lambda_{0,1}^P - \alpha\lambda_{0,1}^E + \beta\lambda_{0,0}^E$ $\frac{d\lambda_{1,0}^E}{dt} = k_{i1}C_2E_S + \gamma\lambda_{1,0}^P + (\beta - k_{11}E_S)\lambda_{0,0}^E - \alpha\lambda_{1,0}^E$ $\frac{d\lambda_{1,1}^E}{dt} = k_{i1}C_2E_S + \gamma(\lambda_{1,1}^P + \lambda_{0,1}^P) + k_{11}E_S\lambda_{0,1}^E - \alpha\lambda_{1,1}^E + \beta\lambda_{0,0}^E$ $\frac{d\lambda_{2,0}^E}{dt} = k_{i1}C_2E_S + \gamma(\lambda_{2,0}^P + \lambda_{0,0}^P + 2\lambda_{1,0}^P) + k_{11}E_S(\lambda_{0,0}^E + 2\lambda_{1,0}^E) - \alpha\lambda_{2,0}^E + \beta\lambda_{0,0}^E$ $\frac{d\lambda_{0,2}^E}{dt} = k_{i1}C_2E_S + \gamma\lambda_{0,2}^P - \alpha\lambda_{0,2}^E + \beta\lambda_{0,0}^E$
Live copolymer chains with a propylene unit at the end	$\frac{d\lambda_{0,1}^P}{dt} = k_{i2}C_2P_S + k_{12}P_S(\lambda_{0,1}^E + \lambda_{0,0}^E) + (k_{22}P_S + \phi)\lambda_{0,0}^P + k_{tr12}P_S\lambda_{0,0}^E - (\gamma + \varepsilon)\lambda_{0,1}^P$ $\frac{d\lambda_{1,0}^P}{dt} = k_{i2}C_2P_S + k_{12}P_S\lambda_{1,0}^E - (\gamma + \varepsilon)\lambda_{1,0}^P + k_{tr12}P_S\lambda_{0,0}^E + \phi\lambda_{0,0}^P$ $\frac{d\lambda_{1,1}^P}{dt} = k_{i2}C_2P_S + k_{12}P_S(\lambda_{1,1}^E + \lambda_{1,0}^E) + k_{22}P_S\lambda_{1,0}^P - (\gamma + \varepsilon)\lambda_{1,1}^P + k_{tr12}P_S\lambda_{0,0}^E + \phi\lambda_{0,0}^P$ $\frac{d\lambda_{2,0}^P}{dt} = k_{i2}C_2P_S + k_{12}P_S\lambda_{2,0}^E - (\gamma + \varepsilon)\lambda_{2,0}^P + k_{tr12}P_S\lambda_{0,0}^E + \phi\lambda_{0,0}^P$ $\frac{d\lambda_{0,2}^P}{dt} = k_{i2}C_2P_S + k_{12}P_S(\lambda_{0,2}^E + \lambda_{0,0}^E + 2\lambda_{0,1}^E) + k_{22}P_S(\lambda_{0,0}^P + 2\lambda_{0,1}^P) - (\gamma + \varepsilon)\lambda_{0,2}^P + k_{tr12}P_S\lambda_{0,0}^E + \phi\lambda_{0,0}^P$
Dead copolymer chains	$\frac{d\mu_{0,1}}{dt} = \varepsilon(\lambda_{0,1}^E + \lambda_{0,1}^P) + (k_{tr12} + k_{ter12})P_S(\lambda_{0,0}^E + \lambda_{0,0}^P)$ $\frac{d\mu_{1,0}}{dt} = \varepsilon(\lambda_{1,0}^E + \lambda_{1,0}^P)$ $\frac{d\mu_{1,1}}{dt} = \varepsilon(\lambda_{1,1}^E + \lambda_{1,1}^P) + (k_{tr12} + k_{ter12})P_S(\lambda_{1,0}^E + \lambda_{1,0}^P)$ $\frac{d\mu_{2,0}}{dt} = \varepsilon(\lambda_{2,0}^E + \lambda_{2,0}^P)$ $\frac{d\mu_{0,2}}{dt} = \varepsilon(\lambda_{0,2}^E + \lambda_{0,2}^P) + (k_{tr12} + k_{ter12})P_S[\lambda_{0,0}^E + \lambda_{0,0}^P + 2(\lambda_{0,1}^E + \lambda_{0,1}^P)]$

$$\alpha = k_{trAl}\left(\frac{Al_0}{C_{10}} - 1\right)Al_0 + k_{tr1H}H_S + k_{ter1} + (k_{12} + k_{tr12} + k_{tr12})P_S$$

$$\beta = k_{trAl}\left(\frac{Al_0}{C_{10}} - 1\right)Al_0 \quad \gamma = k_{21}E_S$$

$$\varepsilon = k_{trAl}\left(\frac{Al_0}{C_{10}} - 1\right)Al_0 + k_{tr1H}H_S + k_{ter1} + (k_{tr12} + k_{tr12})P_S$$

$$\phi = k_{trAl}\left(\frac{Al_0}{C_{10}} - 1\right)Al_0 + k_{tr12}P_S \quad (15)$$

The concentration of dead polymeric chains in the reactor was controlled by transfer and termination reactions, which happened for both kinds of live polymeric chains, those with propylene at the end ( $P_{ij}$ ) and those with ethylene at the end ( $E_{ij}$ ):

$$\frac{d\mu_{0,0}}{dt} = \varepsilon(\lambda_{0,0}^E + \lambda_{0,0}^P) \quad (16)$$

Population balance was defined for all active species in the reactor. Table III shows the different orders of these equations for the live and dead polymeric chains.

By computing the amount of these moments at any instance, we were able to calculate the number-average molecular weight ( $M_n$ ) and weight-average molecular weight ( $M_w$ ), PDI, and the ethylene content of the copolymer with the following equations:

$$\langle X_{n,1} \rangle = \frac{\mu_{1,0} + \lambda_{1,0}^E + \lambda_{1,0}^P}{\mu_{0,0} + \lambda_{0,0}^E + \lambda_{0,0}^P} \quad (17)$$

$$\langle X_{n,2} \rangle = \frac{\mu_{0,1} + \lambda_{0,1}^E + \lambda_{0,1}^P}{\mu_{0,0} + \lambda_{0,0}^E + \lambda_{0,0}^P} \quad (18)$$

$$\langle X_n \rangle = \langle X_{n,1} \rangle + \langle X_{n,2} \rangle \quad (19)$$

$$\bar{M}_n = M_E \langle X_{n,1} \rangle + M_P \langle X_{n,2} \rangle \quad (20)$$

$$\langle X_{W,1} \rangle = \frac{M_E(\mu_{2,0} + \lambda_{2,0}^E + \lambda_{2,0}^P) + M_P(\mu_{1,1} + \lambda_{1,1}^E + \lambda_{1,1}^P)}{M_E(\mu_{1,0} + \lambda_{1,0}^E + \lambda_{1,0}^P) + M_P(\mu_{0,1} + \lambda_{0,1}^E + \lambda_{0,1}^P)} \quad (21)$$

$$\langle X_{W,2} \rangle = \frac{M_E(\mu_{1,1} + \lambda_{1,1}^E + \lambda_{1,1}^P) + M_P(\mu_{0,2} + \lambda_{0,2}^E + \lambda_{0,2}^P)}{M_E(\mu_{1,0} + \lambda_{1,0}^E + \lambda_{1,0}^P) + M_P(\mu_{0,1} + \lambda_{0,1}^E + \lambda_{0,1}^P)} \quad (22)$$

$$\langle X_W \rangle = \langle X_{W,1} \rangle + \langle X_{W,2} \rangle \quad (23)$$

$$M_w = M_E \langle X_{W,1} \rangle + M_P \langle X_{W,2} \rangle \quad (24)$$

$$\langle F_1 \rangle = \frac{\langle X_{n,1} \rangle}{\langle X_n \rangle} \quad (25)$$

$$\langle F_2 \rangle = \frac{\langle X_{n,2} \rangle}{\langle X_n \rangle} \quad (26)$$

where  $\langle X_{W,1} \rangle$ ,  $\langle X_{W,2} \rangle$  and  $\langle X_w \rangle$  are weight-average and  $\langle X_{n,1} \rangle$ ,  $\langle X_{n,2} \rangle$  and  $\langle X_n \rangle$  are number average degrees of polymerization of ethylene, propylene and copolymer, respectively.  $M_H$  and  $M_P$  are molecular weights of ethylene and propylene, respectively.  $\langle F_1 \rangle$  and  $\langle F_2 \rangle$  denote the ethylene and propylene contents, respectively, in the copolymer.

PDI and polymer yield or concentration in the reaction medium ( $Y_p$ ) were obtained from the following equations:

$$PDI = \frac{M_w}{M_n} = \frac{\langle X_w \rangle}{\langle X_n \rangle} \quad (27)$$

$$Y_p = \mu_{0,0} M_n \quad (28)$$

The total rate of copolymerization ( $R_p$ ) was defined as follows:

$$R_p = \left( -\frac{dM_1}{dt} \right) + \left( -\frac{dM_2}{dt} \right) \quad (29)$$

$$R_p = (k_{i1}C_2 + k_{11}\lambda_{0,0}^E + k_{21}\lambda_{0,0}^P)E_S + [k_{i2}C_2 + (k_{12} + k_{ter12})\lambda_{0,0}^E + k_{22}\lambda_{0,0}^P]P_S + k_{ter1}\lambda_{0,0}^E \quad (30)$$

## Energy balance

Energy balance was measured as described by Hagg et al.<sup>6</sup>

## RESULTS AND DISCUSSION

### Kinetic rate constants

The objective function for error minimization [ $f(\text{error})$ ] was defined as the difference between the ethylene

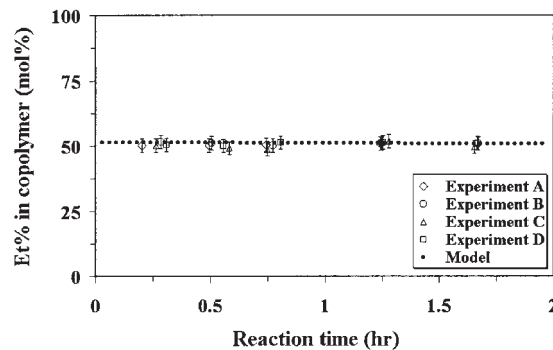


**Figure 2** Comparison of the model calculations with the experimental results for the variation of copolymer ethylene content with reaction time under the experimental conditions given in Table I.

content experimentally determined by  $^{13}\text{C}$ -NMR ( $Et_{\text{EXPi}}$ ) and the corresponding computed value ( $Et_{\text{CALi}}$ ):

$$f(\text{error}) = \sum_{i=1}^{n=18} (Et_{\text{EXPi}} - Et_{\text{CALi}})^2 \quad (31)$$

$^{13}\text{C}$ -NMR<sup>10–14</sup> and IR<sup>5</sup> results determined the monomer reactivity ratios ( $r_1$  and  $r_2$ ). By means of these data, the four kinetic rate constants of propagation step reduced to two rate constants. Then, we estimated the nine kinetic rate constants for the initiation, propagation, transfer, and termination steps by fitting the 18 experimental data of ethylene content in the copolymer (see Fig. 2) and simultaneously solving the equations by the finite difference method with the Marquat optimization procedure as nonlinear equations.<sup>32</sup>

The dynamic model is able to reproduce experimental data for reaction rate, weight-average molecular weight within experimental accuracy with estimated kinetic rate constants. This consequence demonstrates the model validity.

Table IV shows the kinetic rate constants deduced from the proposed model in comparison with the literature. The activation constant was not considered because activated and aged catalysts were used. As indicated by other authors,<sup>1,3</sup>  $k_{11}$  calculated by present model proved that the ethylene–ethylene addition constant was the highest rate constant in the propagation step, and it necessitated control of the reactor feeding to obtain the desired ethylene content in the copolymer.

Compared with  $k_{tr1A1}$  and  $k_{tr12}$ , the higher value of  $k_{tr1H}$  indicated that transfer to hydrogen controlled chain growth. The effect of hydrogen very often transcends that of a mere chain-transfer agent because it can affect the polymerization rate and polymer micro-

TABLE IV  
Comparison of the Kinetic Rate Constants from the Literature with Those of This Model

Reaction step		Constant (mol L <sup>-1</sup> min <sup>-1</sup> )	Cozewith <sup>3</sup> (30°C)	Present model (22°C)	Podolnyi et al. (1963; 20°C)
Activation		$k_a$	166	—	$\infty$
Chain initiation	Ethylene	$k_{i1}$	8.33	13.456	2.0
	Propylene	$k_{i2}$	8.33	2.021	—
Chain propagation	Ethylene	$k_{11}$	23,000	102,175 ± 3325	130,000
		$k_{12}$	11,000	4,400	13,000
	Propylene	$k_{21}$	14,200	12,305 ± 455	11,000
		$k_{22}$	1,330	184 ± 66	316
Chain transfer	Propylene	$k_{tr12}$	0.133	21.2	—
	Al-alkyl	$k_{tr1A1}$	—	0.012	—
	Hydrogen	$k_{tr1H}$	1,200	3457	—
Chain termination	Catalyst deactivation	$k_{ter1}$	0.035	14.2	19
	Propylene	$k_{ter12}$	1.466	0.45	0

structure significantly.<sup>23,24</sup> Because all of these chain-transfer agents (hydrogen, propylene, and alkyl aluminum) were present in the experimental system, the obtained data were able to predict the effect of chain transfer by hydrogen ( $k_{tr1H}$ ), propylene ( $k_{tr12}$ ), and alkyl ( $k_{tr1A1}$ ).

According to the models proposed in the literature, the chain termination step can occur only by spontaneous catalyst deactivation or with propylene monomer. These reactions also occur with live chains. Identical reactions occur with growing  $P_{ij}$  chains to produce dead chains. Termination and transfer constants are assumed to be the same regardless of the chain end type.<sup>4,6</sup>

Another parameter that affects the kinetic rate constants is the temperature of polymerization. The data in this study (22°C) was different from those reported by Podolnyi et al.<sup>1</sup> and Cozewith<sup>4</sup> because, in their investigations, polymerization was carried out at 20 and 30°C, respectively. By comparing the different results of these studies, we observed a coherence for each kinetic constant, except for  $k_{i1}$ ,  $k_{i2}$ ,  $k_{12}$ , and  $k_{22}$ . These differences may have been due to hydrogen effects as a chain-transfer agent and because the initiation step started with both monomers at different rates.

### Copolymer composition

As shown in Figure 2, the ethylene content of the copolymer was constant during the polymerization time. This composition homogeneity was an outcome of the constant concentration of the monomers due to the initial saturation of solvent with monomers and the high mass-transfer rates of the monomers, which satisfied the steady monomer concentration during the reaction. These observations were also supported by other works reported in the literature.

### Reaction rate

Figure 3 shows that the predictions of this model agreed well with the experimental reaction rate data for a long reaction time. This accuracy resulted by the application of a double moments equation for the two reactants.

### Molecular weight

As shown in Figure 4, the molecular weight growth of the copolymer calculated by this model was in good agreement with the experimental data. The initial period in olefin polymerization is often characterized by a gradual increase in the polymer molecular weight up to some constant value. This behavior is typical of olefin polymerization carried out at moderate temperatures (<50°C) and low monomer concentrations in the presence of highly active catalytic systems.<sup>28</sup> The initial increase of molecular weight is approximately regarded as quasiliving chain growth. When reaction rate of chain initiation and chain termination reach equilibrium, molecular

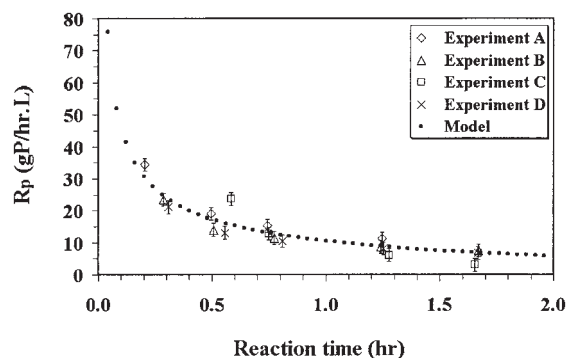


Figure 3 Comparison of the model predictions with the experimental results for the variation of  $R_p$  with reaction time under the experimental conditions given in Table I.



weight is independent of the time under stationary conditions. If the process is carried out at relatively low temperatures, molecular weight growth can be observed even for a few hours. At high polymerization temperatures (70–80°C) and high monomer concentrations, the stage of molecular weight time independence appears in a shorter period of time. A detailed description of these phenomena was described by Kissin.<sup>28</sup>

The use of hydrogen as a molecular weight controlling agent is shown in Figure 5. Molecular weight approached a plateau limit for the hydrogen chain-transfer ability. This behavior was attributed to a lower magnitude for the rate constant of chain transfer by hydrogen than the average of propagation rate constants.

Also, alkyl chain-transfer effects were taken into consideration in the polymerization kinetics when the Al/V ratio was varied from 2 to 64. For Al/V ratios lower than 2, no significant yield was obtained. At least two alkyl aluminum molecules and one vanadium salt were required to form the active species.<sup>6,33</sup> The alkyl chain-transfer effect on molecular weight was intensified by excess alkyl when an Al/V ratio ( $\approx 28$ ) higher than the optimum value ( $\approx 8$ ) was used, as indicated by the experimental data and model predictions.

## CONCLUSIONS

A dynamic model based on double moments was developed to describe the effects of hydrogen and an Al/V ratio up to 28 on the reaction rate, molecular weight, and composition of the copolymer in ethylene-propylene copolymerization with a vanadium-based Ziegler-Natta catalyst. The dynamic model was able to reproduce the experimental data within experimental accuracy for a long reaction time. This model accurately demonstrated the fundamental importance

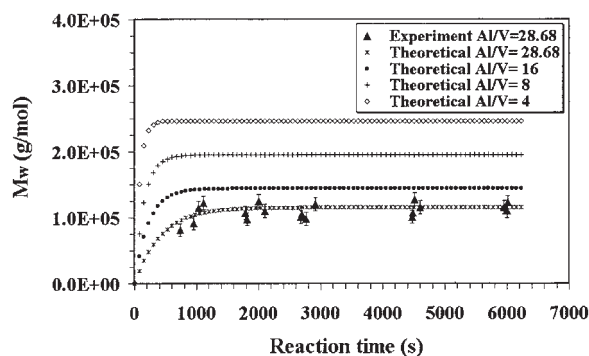


**Figure 4** Comparison of the model predictions with the experimental results for the variation of copolymer molecular weight with reaction time under the experimental conditions given in Table I.

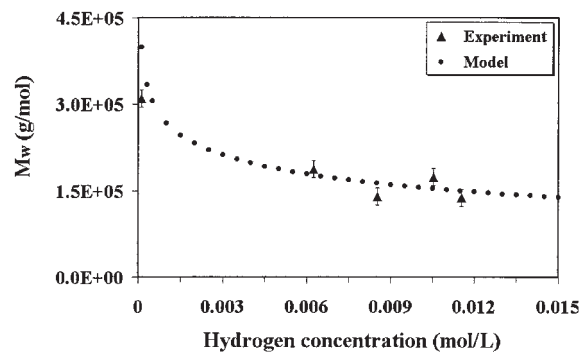


**Figure 5** Comparison of the model predictions with the experimental results for the variation of hydrogen effect on copolymer molecular weight (Al/V = 8.314,  $\text{VOCl}_3 = 7.2 \times 10^{-5}$  mol/L, time = 5400 s, [ethylene] = 0.04838 mol/L, [propylene]/[ethylene] = 10.988, temperature = 22°C).

of polymerization variables on the final properties of the polymer material in the copolymerization of ethylene and propylene with Al/V ratios up to 28 before synthesis. The success of the model was an outcome of the application of a double moments equation for the two reactants.

## NOMENCLATURE

$Al, Al_0$  Initial and corrected alkyl aluminum concentrations (mol/L)

$a_E, a_P, a_H$  Ethylene, propylene, and hydrogen interfacial specific areas ( $\text{m}^2/\text{m}^3$ )

$C_{10}, C_1, C_2$  Vanadium and active species concentrations (mol/L)

$D$  Deactivated catalyst species concentration (mol/L)

PDI Polydispersity index

$E_{EQ}, E_F, E_G, E_{GS}, E_S$  Ethylene concentrations at equilibrium, in the feed, in the gas phase, at gas out, and solved in the liquid phase (mol/L)

$\langle F_1 \rangle, \langle F_2 \rangle$  Ethylene and propylene contents in the copolymer

$F_E, F_P, F_H, F_G, F_R$  Volumetric flow rates of ethylene, propylene, hydrogen, the gas phase, and the cooling liquid (L/min)

$H_{EQ}, H_F, H_G, H_{GS}, H_S$  Hydrogen concentrations at equilibrium, in the feed, in the gas phase, at gas out, and solved in the liquid phase (mol/L)

$k_l$  Mass-transfer coefficient based on the liquid phase for ethylene, propylene, or hydrogen ( $\text{min}^{-1}$ )

$M_n, M_w$  Number- and weight-average molecular weights (g/mol)

$P_{SET}$ , set point and reactor pressures (bar)

$P_{EQ}, P_F, P_G, P_{GS}, P_S$  Propylene concentrations at equilibrium, in the feed, in the gas phase, at gas out, and solved in the liquid phase (mol/L)

$R_p$  Rate of the copolymerization reaction  
 $V_G, V_L$  Gas phase and liquid phase volume (L)  
 $Y_p$  Polymer yield or concentration in the reaction medium (g/L)

### Greek characters

$\alpha, \beta, \gamma, \varepsilon, \phi$  Mathematical variables of the model  
 $\lambda_{0,0}^E, \lambda_{0,1}^E, \lambda_{1,0}^E, \lambda_{1,1}^E, \lambda_{2,0}^E, \lambda_{0,2}^E$  Activated ethylene units with different orders of double moments for live chains terminated with ethylene (mol/L)  
 $\lambda_{0,0}^P, \lambda_{0,1}^P, \lambda_{1,0}^P, \lambda_{1,1}^P, \lambda_{2,0}^P, \lambda_{0,2}^P$  Activated propylene units with different orders of double moments for live chains terminated with propylene (mol/L)  
 $\mu_{0,0}, \mu_{0,1}, \mu_{1,0}, \mu_{1,1}, \mu_{2,0}, \mu_{0,2}$  Different orders of double moments for all of the dead chains (mol/L)

### References

- Podolnyi, Y. B.; Solovyeva, G. V.; Kamenev, Y. G. *Polym Sci USSR* 1974, 16, 2767.
- Pronyaev, V. N.; Afanasev, I. D.; Kovaleva, G. A. *Polym Sci USSR* 1985, 27, 1292.
- Cozewith, C. Proceedings of the 73rd AIChE meeting, Chicago, American Institute of Chemical Engineers, Nov 16–20, 1980.
- Cozewith, C. *AIChE J* 1988, 34, 272.
- Cozewith, C.; Ver Strate, G.; Ju, S. *Macromolecules* 1988, 21, 3360.
- Haag, M. C.; Dos Santos, J. H. Z.; Dupont, J.; Secchi, A. R. *J Appl Polym Sci* 1998, 70, 1173.
- da Silva Filho, A. A.; de Galland, G. B.; Soares, J. B. P. *Macromol Chem Phys* 2000, 201, 1226.
- Soares, J. B. P. *Chem Eng Sci* 2001, 56, 4131.
- Latado, A.; Embiruçu, M.; Mattos Neto, A. G.; Pinto, J. C. *Polym Test* 2001, 20, 419.
- Kapur, G. S.; Sarpal, A. S.; Mazumdar, S. K.; Jain, S. K.; Srivastava, S. P.; Bhatnagar, A. K. *Lub Sci* 1995, 8 (Oct), 49.
- Martino, S. D.; Kelchtermans, M. *J Appl Polym Sci* 1995, 56, 1781.
- Kolbert, A. C.; Didier, J. G. *J Appl Polym Sci* 1999, 71, 523.
- Debling, J. A.; Han, G. C.; Kuijpers, F.; Verburg, J.; Zacca, J.; Ray, H. *AIChE J* 1994, 40, 506.
- Soares, J. B. P.; Hamielec, A. E. *Makromol Theor Simul* 1995, 4, 1085.
- de Carvalho, A. B.; Gloor, P. E.; Hamielec, A. E. *Polymer* 1989, 30, 280.
- Galvan, R.; Tirrell, M. *Chem Eng Sci* 1986, 41, 2385.
- Keii, T. *Macromol Theor Simul* 1995, 4, 947.
- Natta, G.; Mazzanti, G.; Valvassori, A.; Sartori, G.; Barbagallo, A. *J Polym Sci* 1961, 51, 429.
- Chen, C. M.; Ray, W. H. *J Appl Polym Sci* 1993, 49, 1573.
- Jaber, I. A.; Ray, W. H. *J Appl Polym Sci* 1993, 49, 1709.
- Haag, M. C.; Krug, C.; Dupont, J.; Galland, G. B.; Dos Santos, J. H. Z.; Uozumi, T.; Sano, T.; Soga, K. *J Mol Catal Chem: A* 2001, 169, 275.
- McKenna, T. F.; Soares, J. B. P. *Chem Eng Sci* 2001, 56, 3931.
- Soares, J. B. P.; Hamielec, A. E. *Polymer* 1996, 37, 4606.
- Soares, J. B. P.; Hamielec, A. E. *Polymer* 1996, 37, 4599.
- Valvassori, A.; Sartori, G.; Mazzani, G.; Pajaro, G. *Makromol Chem* 1963, 61, 46.
- Yiagopoulos, A.; Yiannoulakis, H.; Dimos, V.; Kiparissides, C. *Chem Eng Sci* 2001, 56, 3979.
- Treybal, R. *Mass Transfer Operations*, 3rd ed.; McGraw-Hill: New York, 1980; Chapter 6, p 139.
- Kissin, Y. V. *Isospecific Polymerization of Olefins with Heterogeneous Ziegler-Natta Catalysts*; Springer-Verlag: New York, 1985; p 1.
- Holderbaum, T.; Gmehling, J. *Fluid Phase Equilib* 1991, 70, 251.
- Fischer, K.; Gmehling, J. *Fluid Phase Equilib* 1995, 112, 1.
- Stephen, H.; Stephen, T. *Solubilities of Inorganic and Organic Compounds*; Pergamon Press: Oxford, 1963; p 1179.
- Edgar, T. F.; Himmelblau, D. M. *Optimization in Chemical Processes*; McGraw-Hill: New York, 1989; p 214.
- Baldwin, F. P.; Ver Strate, G. *Rubber Chem Technol* 1972, 45, 709.